Modeling rainfall diurnal variation of the North American monsoon core using different spatial resolutions

Jialun Li, X. Gao, K.-L. Hsu, B. Imam, and S. Sorooshian

Department of Civil and Environmental Engineering, University of California, Irvine, Irvine, CA 92697-2175

Extended abstract for 27th Conference on Hurricanes and Tropical Meteorology,
Monterey, California, 24-28 April 2006

Corresponding author address:

Jialun Li

Department of Civil and Environmental Engineering

E-4130 Engineering Gateway

The University of California, Irvine

Irvine, CA 92697-2175

Email: jialunl@uci.edu

ABSTRACT

Rainfall diurnal variation is one of the important components in the North American Monsoon System (NAMS). In this study this component is numerically studied using the mesoscale model NCAR/PENN STATE MM5 with different resolutions (27, 9, and 3 –km grids). The model was initialized every two days using Eta AWIP data.

The result from 3-km resolution indicated that the rainfall variation from monthly, daily to hourly scale was relatively well represented in comparison with that from relatively coarse resolution (such as 27 or 9 -km resolution). However, whichever spatial resolution was used, the model rainfall diurnal variation was underrepresented in intensity and over-represented in frequency in comparison with observations. Rainfall begins earlier over high elevation area than over low elevation area because of solar heating. The outflow from relatively earlier time and higher elevation locations is responsible for the rainfall storms in the later time and lower elevation areas.

1. Introduction

Previous studies have indicated that diurnal variations of rainfall are one of the features of the North American monsoon system (NAMS). The diurnal cycle of monsoon rainfall has been studied with rain-gauge data (Douglas et al., 1993; Higgins et al., 1999; Gochis et al. 2004) and satellite rainfall estimates (Negri et al., 1993, 1994; Sorooshian et al. 2002). Negri et al. (1993, 1994) identified diurnal cycles of rainfall along the western coast of Mexico: convective storms occur offshore during the early morning hours, with several local maxima around concave-shaped areas of the coastline. During the afternoon and evening period, deep convection reaches its highest development over land with marked maxima along the western slope of the Sierra Madre Occidental (SMO). By analyzing the North American Monson Experiment (NAME) Event Rain gauge Network (NERN) data, Gochis et al (2004) found that the monsoon core rainfall timing and intensity varied with the height of elevation over western Mexico. In this study, using a numerical model, we will try to reproduce this feature in which Gochis et al (2004) has found.

Numerical studies of NAMS have the advantage of high time and space resolution. Anderson et al. (2001) reproduced the LLJ variation from the northern Gulf of California to southwest Arizona using the National Center of Environmental Prediction (NCEP)-Regional Spectral Model (RSM) with 10 km by 20 km horizontal grids. Stensrud et al. (1995) reproduced the observed convective diurnal variations over the western slope of the SMO in MM4 simulations enhanced by the special observational data using 25 km by 25 km horizontal grids and initializing the model every 24 hours. They found that the model overestimated convective frequencies over mountain areas, as well as morning rainfall. Berbery (2001) analyzed three years of forecast precipitation from the NCEP/Eta model (48 km horizontal grids) and found the diurnal rainfall variation over the SMO to be much weaker than the satellite estimates. He argued that these differences are reasonable because the satellite rainfall was estimated from the maximum instantaneous rainfall sampling in the afternoon (the highest rainfall period of a day) and the model forecast is integrated over time. Li et al. (2004), using 12-km spatial resolution, have investigated rainfall diurnal variation over most of monsoon active regions and found the model cannot well reproduce the rainfall diurnal over Arizona and Northern Texas. While the model can in somehow reproduce the rainfall diurnal variation over western Mexico, there existed differences in amount and timing between model result and satellite data. Possibly because of the model spatial resolution issue, no model studies have noticed the timing shift of rainfall diurnal variation with elevations over the SMO.

2. Numerical Modeling

a. Study domain

Three tests were designed and run separately. Test–1: Three nested domains were used in the simulations. Domain 1 covers the western and central U.S., Mexico, and the surrounding oceans with a 27–km horizontal grid mesh (total 148 by 103 grid cells).

Domain 2 covers Mexico, southwestern United States, Texas, Oklahoma, and surrounding water, including the eastern Pacific Ocean, the Gulf of California, and the Gulf of Mexico with a 9-km grid (total 199 by 187 grid cells). Domain 3 is at 3-km resolution and covers the western slope of the SMO and portions of the Gulf of California (total 271 by 286 grid cells). Test–2: the same as Test–1, but only domain 1 and 2 were used. And Test–3: the same as Test-1 but only Domain-1 was used.

Fig. 1 is the scatter plot between the NERN station elevation and model terrain in different resolutions. There were over 80 gauge stations during July and August 2004. Details about the NERN can be found in reference (Gochis et al.2004). This figure indicates that the higher the spatial resolution, the closer the elevation between model and real elevation.

b. Model physics

MM5 provides multiple options and schemes to represent a variety of physical processes. Through our tests, when the Grell CPS (Grell, 1993) was used in DOMAIN 1 and 2, the model produces reasonable rainfall patterns. Thus, the Grell CPS, with the Goddard Space Flight Center (GSFC) explicit cloud microphysical solution (Tao and Simpson, 1989), was used. Additional model physics schemes selected for the study include: MRF boundary layer scheme (Hong and Pan, 1986), and the NOAH land-surface model (Chen and Dudhia, 2001). The vertical coordinate of the MM5 is a terrain-following coordinate system. In this study, thirty vertical sigma layers were employed from surface to the top of atmosphere at 100 mb.

The Eta AWIP data for July and August 2004 was used for model initialization and boundary forcing. The re-initialization was conducted at 0000 UTC on every 2-day and the lateral boundary of domain-1 (D-1) was updated every 12 hours.

c. Rainfall observation data

To evaluate the model results, two independent rainfall data sets are used as references. One is the NCEP 0.25^{o} grid rainfall data (available at http://www.cpc.ncep.noaa.gov/products/precip). The NCEP data is interpolated from daily rain-gauge measurements (hereafter refer to as NCEP gauge data) and covers the continental United States and Mexico. Therefore, it has been used in many NAMS studies (Higgins et al., 1997, 1999; Li et al. 2004). However, it should be noted that, because of the mountainous topography in Mexico and the southwest U.S., the rain gauges in the region are sparse and heterogeneous (more gauges are located in accessible flat valleys than in the mountains), which could affect the accuracy of the rainfall data. NAME event rainfall gauge network (NERN) data (Gochis et al. 2004) were also employed to compare model daily rainfall and diurnal cycles.

3. Results

a. Monthly mean rainfall

Fig. 2 shows mean monthly rainfall distributions for July and August 2004 between observation and simulations from different model runs based on different spatial resolutions. NCEP 25-km gauge data was linearly interpolated onto 27-km resolution just for plotting. The figure indicates that the rainfall distribution and intensity were obviously improved when higher-spatial resolution was used although the model still overestimated rainfall over the southern SMO and underestimated over the northern SMO.

b. Daily rainfall

Fig.3 is the daily rainfall variations between model result and NERN data. The model results are from the grid that is closest to the NERN station and the NERN represents the 85(83) gauges mean in July (August). The results show that the model performed better in July than in August. Also, when 3km resolution was used, the model performed better than when 27-km or 9-km resolution was used, especially in July. However, whichever resolution was used, the model did not reproduce the early and late August NERN rainfall variation.

The authors also compared the rainfall variations of daily time series between NERN and simulations at different transects (figure not shown. During NAME, the NERN gauge equipment was installed in total 6 groups or transects from the most southern SMO, named T-1 to the most northern SMO and called T-6. For each group or transect, many gauges were installed in west-east direction, separately). The result indicates that when 27-km and 9-km spatial resolutions were used, the model severely overestimated the daily rainfall at the most two southern transects (T-1 and T-2, especially at T-1). Moreover, whichever spatial resolution was used, the model underestimated the rainfall during the first few days after monsoon rainfall began.

c. Rainfall Diurnal cycle

(1) Rainfall mean diurnal variation

Fig. 4 is the rainfall mean diurnal cycles between NERN and model grid closest to the gauge station from different elevations as Gochis et al (2004) has classified. The mean hourly amount is equal to the total rainfall amounts divided by integration days. This figure shows that generally, when 3-km spatial resolution was used, the model rainfall diurnal variation matches the observation better than those when 27-km or 9-km resolution was used. Because when 27-km or 9-km resolution was used, the model result has a relatively large deviation in comparison with either NERN data or 3-km resolution model result. It should be noted that there was one exception: the 27-km resolution model result was better when the elevation is between 1000-1500 meters. However, when 3-km resolution was used, the model rainfall always ended earlier than the observation.

Fig. 5 is the spatial distribution of the model mean rainfall peak hour during the integration time period. This figure shows that over the west slope of the SMO, with elevation varying (See Fig. 1) from high elevation, which is close to the continental divide, to the low elevation, which is close to the east coast of the Gulf of California, the rainfall peak hour varied from noon to late afternoon, and even to early evening. The phenomenon is especially clear when higher model spatial resolution was used.

The authors also analyzed the rainfall intensity and frequency and found that, in general, the model over-represented the rainfall frequency and underrepresented the intensity (not shown) whichever resolution was used.

c. The possible mechanism of rainfall diurnal cycle

From Fig. 3, there are two events (~ July 12 to 15 and July 21 to 25) that the model generally well reproduced in daily rainfall evolution. We have analyzed the modeling fields (vertical velocity, rainfall and lower layer wind, potential temperature, and mixing ratio) hourly by hourly for these two events. Fig. 6 shows some selected hourly rainfall evolutions on July 14. The area of Fig. 6 is the box in Fig.2. This figure indicates that rainfall begins at relatively high elevation and far from the Gulf of

California. With time being, the rainfall moves westward toward the Gulf. This rainfall evolution track is common during the simulation period. However, The authors also noticed some other rainfall storm tracks, after the storm occurred at relatively high elevation, it moves northwestward (for example, the afternoon time of July 24) or southeastward (for example, the afternoon time of July 13, and 21) along the west slope of the SMO.

Fig. 7 is the timing evolution of potential temperature and wind vector at the 29th model level ($\sigma = 0.9865$) at some selected time periods. In this figure, the upslope wind (1Z), storm outflow, and outflow cool air (3Z, 5Z, and 7Z) are clearly indicated. This low-level wind and temperature distribution favors triggering the convection. The possible rainfall mechanism could be as follow: at day time, both data analysis (Douglas et al. 1998) and the model result (Anderson et al. 2001; Li et al. 2004) show that there are strong upslope wind, which transport the moist air that evaporates from the Gulf of California, to the west slope of SMO. With solar heating, the convection is triggered first over the high elevation region. Because of terrain features, the cool and outflow air from solar heating convection moves westward, and meets with upslope wind from the Gulf and forces the warm and wet air mass from the Gulf lifting. The new convection next to the high elevation, which is relatively low elevation, is triggered, and so on. Due to the different features of the synoptic scale circulation, as Anderson et al (2001) addressed, there are three types of synoptic circulations during summer monsoon season, the convection over the west slope of SMO does not just move westward.

4. Conclusions

Using a different spatial resolution (27-km, 9-km and 3-km) with a mesoscale model, rainfall variations for July and August 2004 over western Mexico were simulated. The results indicate:

*The model can generally reproduce rainfall pattern in NAM core region on monthly scales but can’t reproduce the day-to-day amounts in detail. This situation was severe in August when the model incorrectly simulated the amount of the rainfall events.

*Model can reproduce mean rainfall diurnal variation. The rainfall diurnal timing was also well simulated. Over the west of slope SMO, in general, rainfall begins earlier over high elevation area than that over low elevation. The outflow from earlier and higher elevation locations is responsible to the rainfall storms in the later and lower elevation area. This phenomenon is especially obvious during weak synoptic time.

***** The model overestimated rainfall frequency while it underestimated rainfall intensity.

Acknowledgements. Primary support for this research was provided under the NASA/EOS Interdisciplinary Research Program (NAG5-11044), NASA/NNG06GB20G, the NOAA GAPP Program (NA16GP1605) and the NSF-STC Program (Agreement EAR-9876800).

References

Anderson, B. T., J. O. Roads, S-C. Chen, and H-M. H. Juang: 2001: Model dynamics of summertime low-level jets over northwestern Mexico. *J. Geophys. Res*., **106(D4)**, 34-1-3413.

Berbery, E. H., 2001: Mesoscale moisture analysis of the North American monsoon. *J. Climate*, **14**, 121-137.

Chen, F., and J. Dudhia, 2001: Coupling an advanced land surface hydrology model with the Penn State-NCAR MM5 modeling system. Part I: Model implementation and sensitivity. *Mon. Wea. Rev*., **129**, 569-585.

Douglas, R. A. Maddox, and K. Howard, 1993: The Mexican monsoon. *J. Climate*, **5**, 1665-1677.

Douglas, M., A. Valdez-Manzanila, and R. G. Cueta, 1998: Diurnal variation and horizontal extent of the low-level jet over the northern Gulf of California. *Mon. Wea. Rev.*, **126**, 2017-2025.

Gochis, D. J., A. Jimenez, C. J. Watts, J. Garatuza-Payan, and W. J. Shuttleworth, 2004: Analysis of 2002 and 2003 warm-season precipitation from the North American monsoon experiment event rainfall gauge network. *Mon. Wea. Rev.*, **132**, 2938-2953.

Grell, G. A., 1993: Prognostic evaluation of assumptions used by cumulus parameterizations. *Mon. Wea. Rev.*, **121**, 764-787.

Higgins, R. W., Y. Chen, and A. V. Douglas, 1999: Interannual variability of the North American warm season precipitation regions. *J. Climate*, **12**, 653-680.

______, Y. Yao, and X. L. Wang, 1997: Influence of the North American monsoon system on the U.S. summer precipitation regime. *J. Climate,* **10**, 2600-2622.

Hong, S-Y. and H-L. Pan, 1996: Nonlocal boundary layer vertical diffusion in a medium-range forecast model. *Mon. Wea. Rev*., **124**, 2322-2339.

Li, J., X. Gao, R. A. Maddox, and S. Sorooshian, 2004: Model study of evolution and diurnal variation of rainfall in the North American monsoon during June and July 2002. *Mon. Wea. Rev*., **132**, 2895 –2915.

Negri, A, R. Adler, and G. Guffman, 1994: Regional rainfall climatologies dericed from Special Sensor Microwave Imager (SSM/I) data. *Bull. Amer. Meteor. Soc.,* **75**, 1165-1182.

______, ______, R. Maddox, K. Howard, and P. Keehn: 1993: A regional rainfall climatology over Mexico and southwest United States derived from passive microwave and geosynchronous infrared data. *J. Climate*, **6**, 2144-2161.

Sorooshian, S., X. Gao, K. Hsu, R. A. Maddox, Y, Hong, H. V. Gupta, and B. Iman, 2002: Diurnal variability of tropical rainfall retrieved from combined GOES and TRMM satellite information. *J. Climate*, **15**, 983-1001.

Stensrud, D. J., R. L. Gall, S. L. Mullen, and K. W. Howard: 1995: Model climatology of the Mexican monsoon. *J. Climate*, **8**, 1775 - 1794.

Tao, W.-K., and J. Simpson, 1989: Modeling of a tropical squall-type convective line. *J. Atmos. Sci.*, **46**, 177–202.

Figure Captions

Fig.1: Terrain scatter plot between NERN station elevation and model output from different resolutions.

Fig. 2: Mean rainfall comparison between model for different resolutions and NECP grid gauge for the two months. The dashed line box in the figure indicates the region for further analysis in text later.

Fig. 3: Daily rainfall time series between NERN data and model grid result closest to the NERN station.

Fig. 4: Mean rainfall diurnal variation at different elevation ranges.

Fig. 5: Model mean rainfall peak hour for the two months.

Fig. 6: Model hourly rainfall (mm) at selected hours in July 14, 2004. The region in this figure covers the region of the dashed line box in Fig. 2.

Fig. 7: The same as Fig.6 but for wind vector and potential temperature (K).

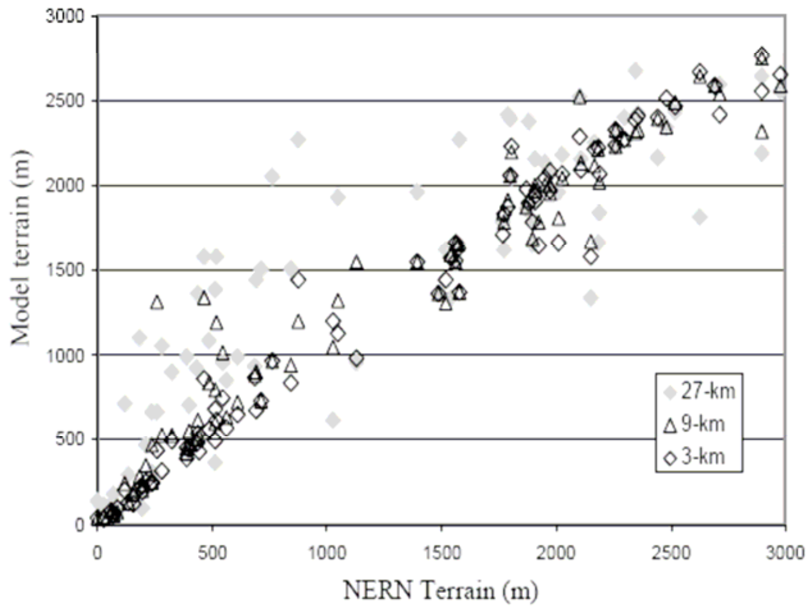

Fig.1. Terrain between NERN station location and model output from different resolutions

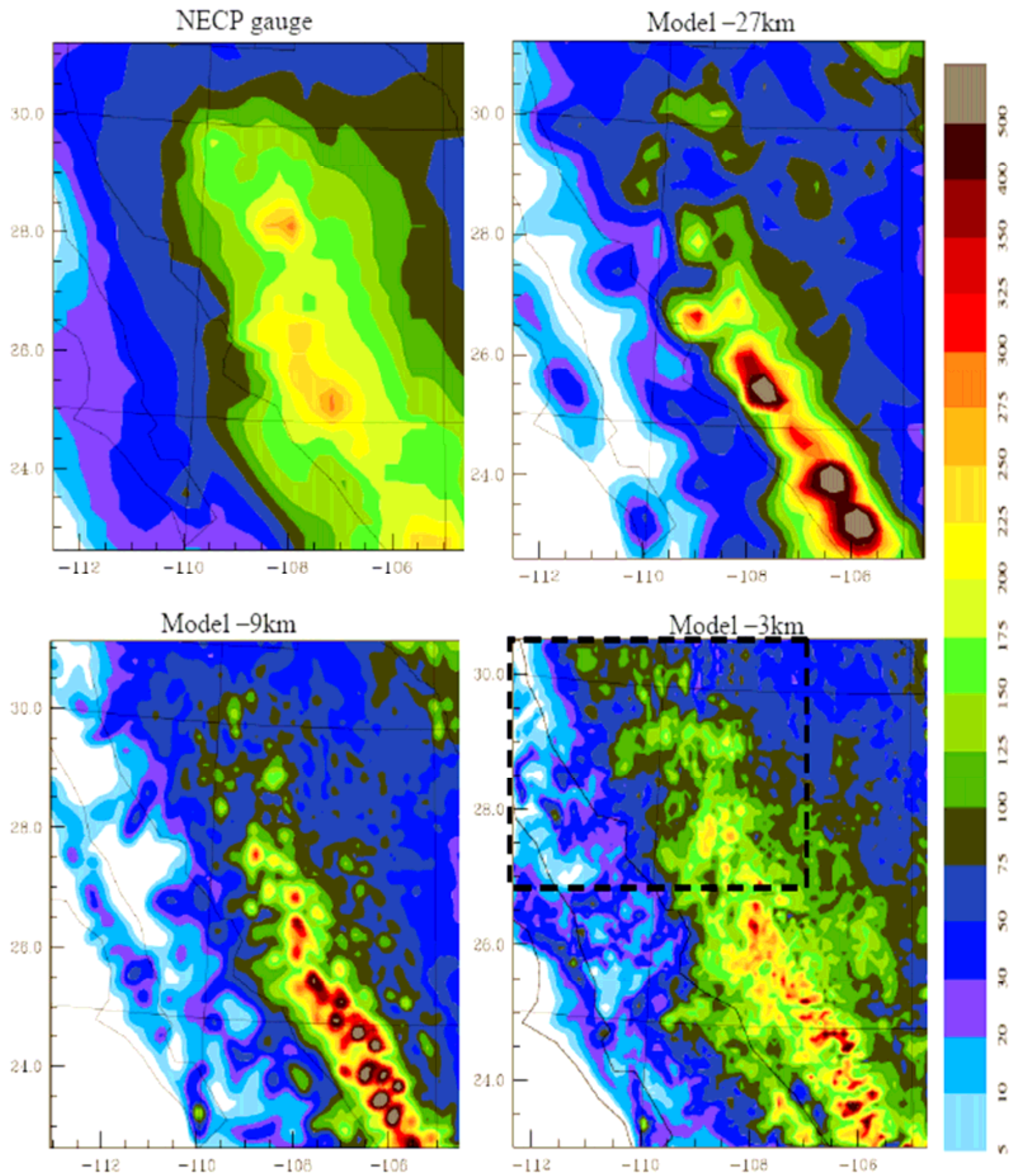

Fig.2. Monthly rainfall distributions at different spatial resolutions. The dashed line box in the figure will be used for further study in the manuscript later.

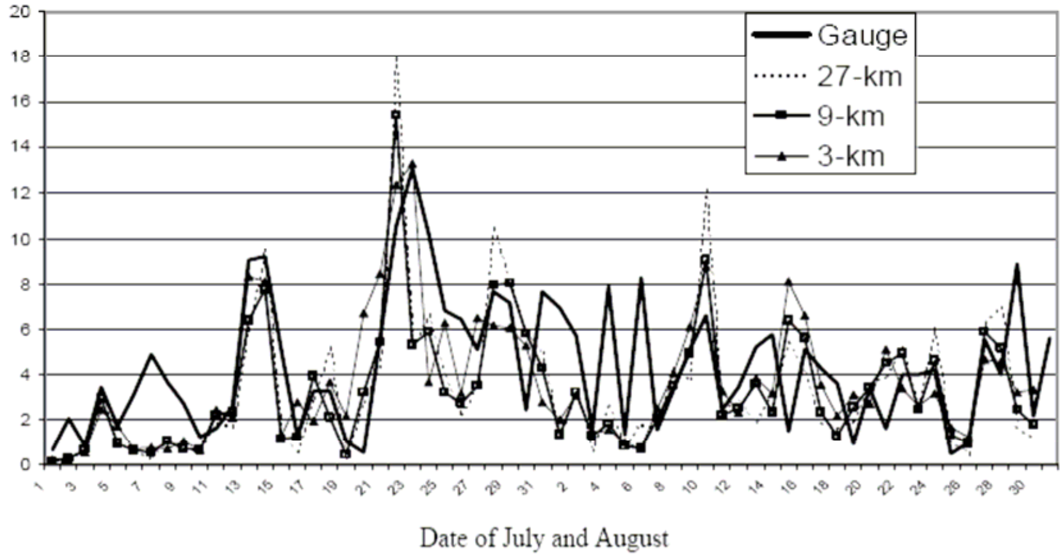

Fig.3. Daily rainfall(mm per day)time series at different spatial resolutions.

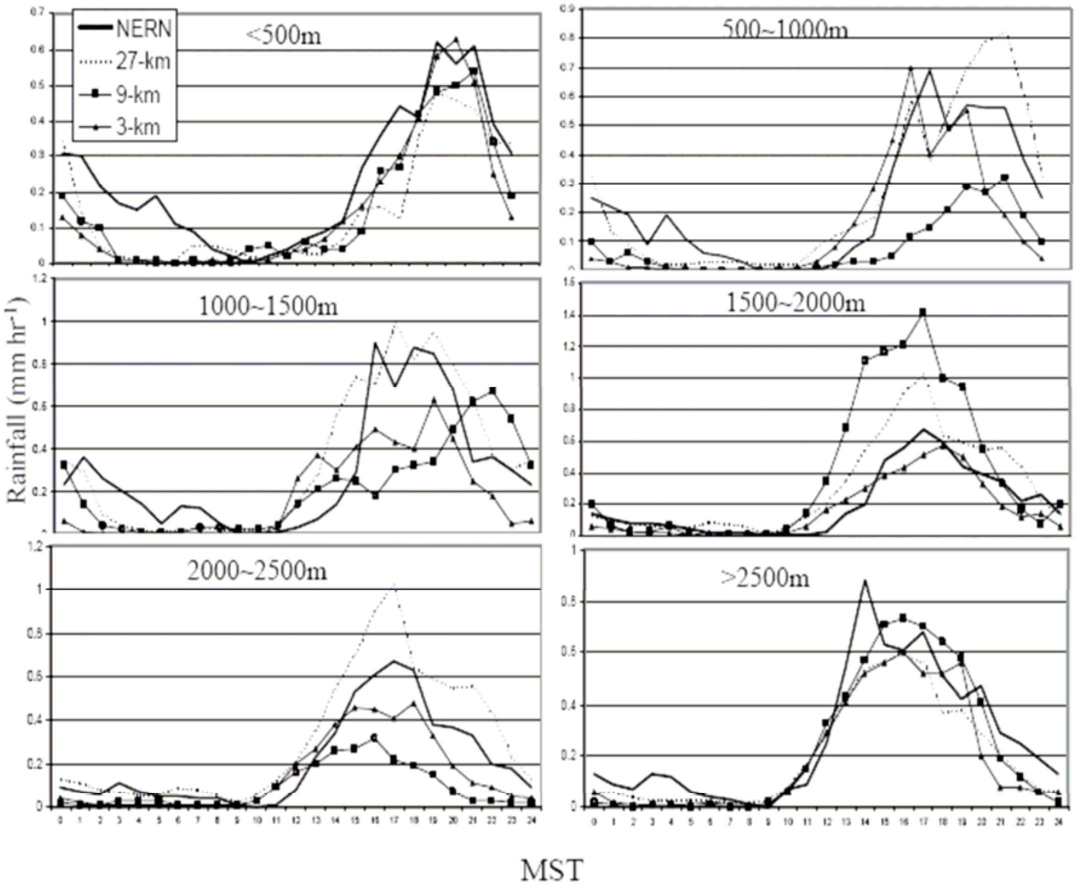

Fig.4. Mean rainfall (mm hr^{-1}) diurnal variation

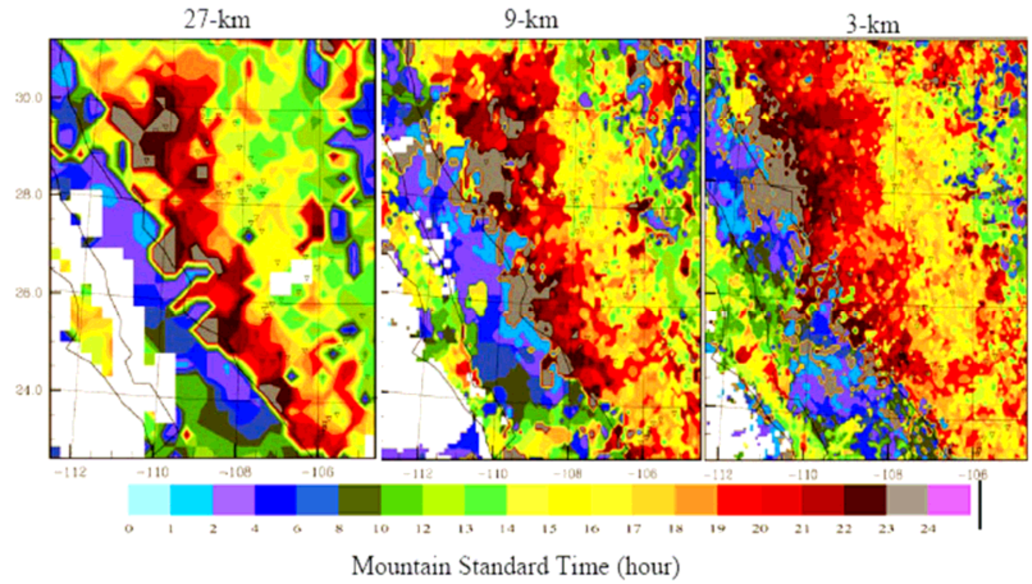

Fig.5. Model mean rainfall peak hour from the two months

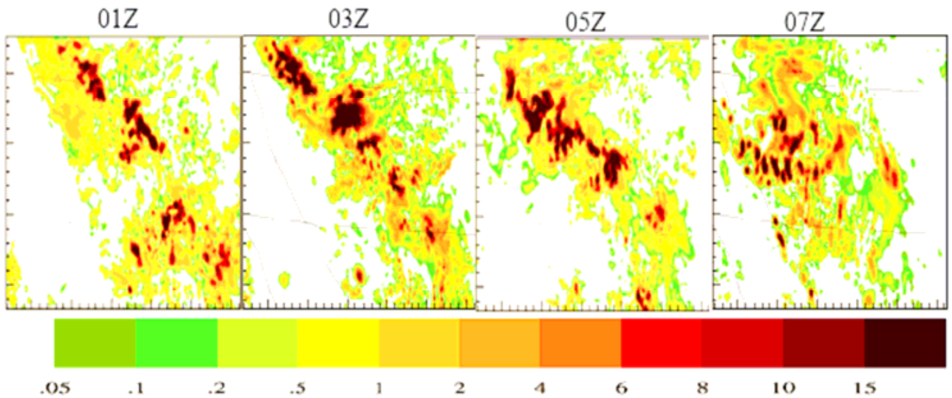

Fig. 6. Model hourly rainfall in July 14, 2004.

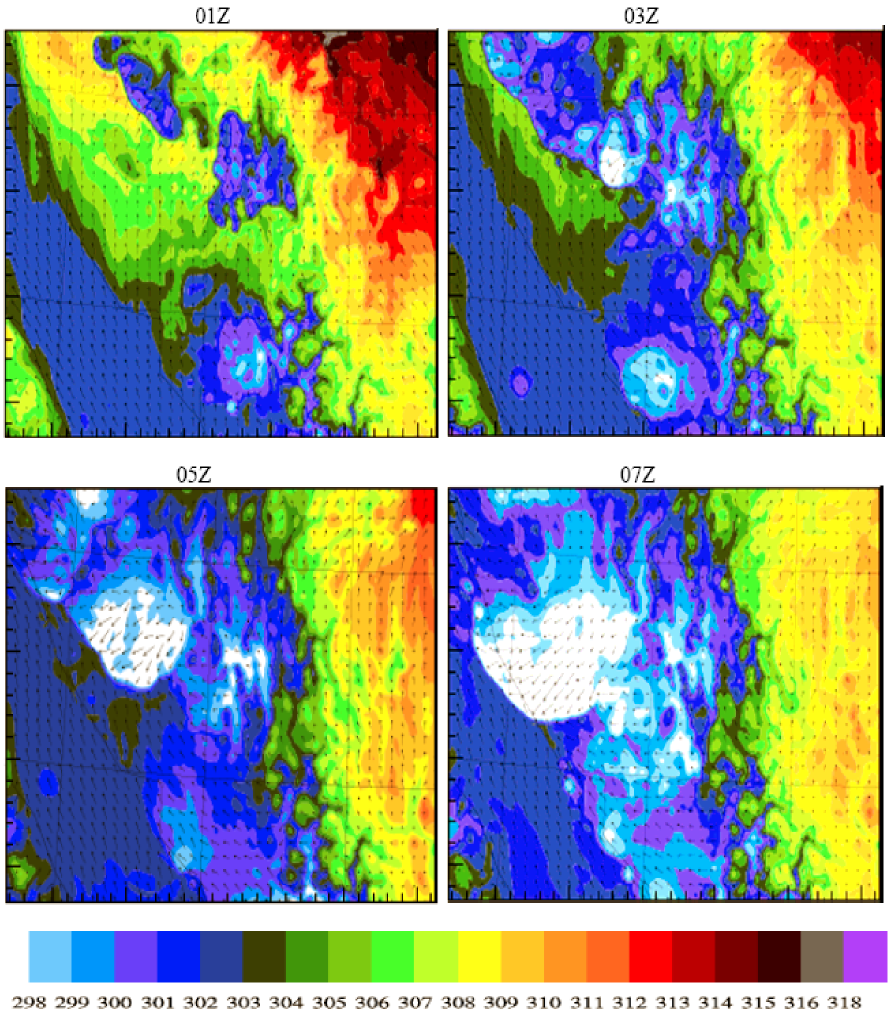

Fig.7. Model wind vector and potential temperature at about 29 vertical layer (about 130m agl) on July 14 2004.